KOREAN JOURNAL OF PACKAGING SCIENCE & TECHNOLOGY
Vol. 32, No. 1 35~43 (2026)
https://doi.org/10.20909/kopast.2026.32.1.35

The Role of Palladium Carbon Quantum Dots on UV-Blocking and Antibacterial Properties of PVA Nanocomposite Films for Food Packaging

Mohammadreza Jozaghkar, Sehyun Jin, Jamilur R. Ansari, and Jongchul Seo*

Department of Packaging, Yonsei University, 1 Yonseidae-gil, Wonju, Kangwon-do, 26493, South Korea

Abstract The development of sustainable and active food packaging materials with multifunctional properties has become increasingly important to enhance food safety and extend shelf life. In this study, palladium-based carbon quantum dots (PQDs) were synthesized via a combined reduction–hydrothermal approach and incorporated into a poly(vinyl alcohol) (PVA) matrix to fabricate multifunctional nanocomposite films. The incorporation of PQDs significantly improved the functional performance of PVA films. UV–Vis analysis revealed excellent ultraviolet shielding, achieving nearly complete blocking in the UV-B region and approximately 90% attenuation in the UV-A region, while maintaining high transparency (>95%) in the visible range. X-ray diffraction results indicated a slight increase in crystallinity without disrupting the intrinsic semi-crystalline structure of PVA. The oxygen transmission rate (OTR) decreased markedly from 5.54 to 0.86 cc/m²·day with increasing PQD content, demonstrating enhanced barrier performance due to the formation of a tortuous diffusion pathway and improved structural ordering. Furthermore, the nanocomposite films exhibited strong antibacterial activity against both *S. aureus* and *E. coli*, with inhibition zones increasing in a concentration-dependent manner. Notably, an inhibition zone of 19.1 mm and 21.9 mm against *S. aureus* and *E. coli*, respectively, was achieved at only 1.0 wt.% PQDs, indicating superior antibacterial efficiency at relatively low filler loadings. The developed PVA/PCQD nanocomposite films demonstrate a unique combination of high transparency, effective UV shielding, improved oxygen barrier properties, and strong antibacterial activity. These findings highlight their potential as advanced, eco-friendly materials for active food packaging applications.

Keywords Palladium Carbon Quantum Dots, Polyvinyl alcohol, Antimicrobial Packaging, Multifunctional Packaging, UV Shielding

Introduction

The widespread use of petroleum-based packaging materials has undeniably improved food preservation and distribution; however, their persistence in the environment has led to severe ecological challenges, particularly long-term plastic accumulation(S. M. Jalilian et al., 2023; Jozaghkar et al., 2026b; M. R. Jozaghkar et al., 2019; Mirtaleb et al., 2025). This growing environmental burden has accelerated the search for sustainable, biodegradable, and high-performance alternatives capable of meeting the functional demands of modern food packaging systems(Jozaghkar et al., 2026a; M. R. Jozaghkar et al., 2022). Among the various candidates, poly(vinyl alcohol) (PVA) has emerged as a promising biodegradable polymer owing to its excellent film-forming ability, transparency, biocompatibility, and superior oxygen-barrier properties. Nevertheless, the intrinsic hydrophilicity of PVA, along with its limited resistance to ultraviolet (UV) radiation and lack of inherent antimicrobial activity, significantly restricts its practical application in active food packaging(Jailani et al., 2026; Saeed and Abdulwahed, 2024).

To address these limitations, the incorporation of functional nanomaterials into polymer matrices has gained considerable attention as an effective strategy to enhance physicochemical and biological properties. In this context, carbon quantum dots (CQDs) have emerged as a versatile class of zero-dimensional nanomaterials, characterized by their small size, large surface area, tunable surface functionalities, and optical properties. CQDs are particularly attractive for food packaging applications due to their excellent dispersibility within polymer matrices, ability to improve UV-shielding performance, and potential antimicrobial activity. Furthermore, their surface chemistry can be readily engineered or doped with heteroatoms or metals to tailor their functionality for specific applications(Gholizadeh et al., 2026; Mahmood et al., 2021; Qiang

*Corresponding Author: Jongchul Seo
Department of Packaging, Yonsei University, 1 Yonseidae-gil, Wonju, Kangwon-do, 26493, South Korea
Tel: +82-31-760-2697
E-mail: jcseo@yonsei.ac.kr

et al., 2020).

Recent advances have highlighted that metal-doped CQDs exhibit significantly enhanced functional properties compared to their undoped counterparts. In particular, palladium (Pd), a noble metal known for its catalytic activity and antimicrobial potential, offers a unique opportunity to engineer CQDs with improved bioactivity and UV-blocking efficiency. Palladium-based carbon quantum dots (PQDs) can introduce additional active sites, facilitate reactive oxygen species (ROS) generation, and disrupt microbial cell membranes, thereby enhancing antibacterial performance. Simultaneously, the incorporation of Pd can modify the electronic structure of CQDs, leading to improved light absorption and UV-shielding capabilities, which are critical for protecting food products from photo-induced degradation(Tang et al., 2025; You et al., 2021).

Despite these promising attributes, the integration of PQDs into biodegradable polymer matrices for food packaging applications remains largely unexplored. Most existing studies have focused on pristine CQDs or other nanofillers such as metal oxides, graphene derivatives, or cellulose-based nanomaterials, often achieving improvements in isolated properties but lacking a balanced enhancement of UV protection, antimicrobial activity, and barrier performance(Elugoke et al., 2024; Li et al., 2019; Qurtulen et al., 2026). Moreover, the potential synergistic effects between PQDs and PVA in creating multifunctional nanocomposite films have not been systematically investigated.

Therefore, this study aims to develop and evaluate multifunctional PVA-based nanocomposite films incorporating palladium-doped carbon quantum dots. It is hypothesized that the incorporation of PQDs will not only improve the UV-blocking performance of PVA films but also impart strong antibacterial activity against common foodborne pathogens, while maintaining desirable mechanical and barrier properties. To validate this hypothesis, nanocomposite films with varying PQD loadings were fabricated and comprehensively characterized in terms of their structural, optical, thermal, mechanical, and antimicrobial properties. The findings of this work are expected to provide new insights into the design of advanced, eco-friendly, and active packaging materials for sustainable food preservation.

Materials and Methods

1. Materials

Poly(vinyl alcohol) (PVA, degree of hydrolysis ~98-99%) and poly(vinyl pyrrolidone) (PVP, $M_w \approx 40{,}000$) were purchased from Sigma-Aldrich (USA). Palladium powder (Pd, ≥ 99.9%) was obtained from Alfa Aesar (USA). Sodium borohydride ($NaBH_4$, ≥98%) was supplied by Daejung Chemicals (South Korea). All chemicals were used as received without further purification. Deionized (DI) water was used throughout all experiments.

2. Synthesis of PQDs

PQDs were synthesized via a combined chemical reduction and hydrothermal approach. Initially, a poly(vinyl pyrrolidone) (PVP) solution (0.05 M) was prepared by dissolving an appropriate amount of PVP in 100 mL of distilled water under magnetic stirring until a clear homogeneous solution was obtained. Subsequently, 5 mL of the prepared PVP solution was withdrawn and used as the solvent medium for further reactions.

For the preparation of the palladium precursor solution, palladium powder (corresponding to a concentration of 0.05 M) was dispersed into 95 mL of the previously prepared PVP solution and stirred continuously to ensure uniform distribution. In parallel, a reducing agent solution was prepared by dissolving 3.78 mg of sodium borohydride ($NaBH_4$) in the 5 mL aliquot of PVP solution. The reduction process was initiated by adding the freshly prepared $NaBH_4$ solution dropwise into the palladium precursor solution under constant stirring. The reaction mixture was maintained at 80°C for 3 h to facilitate the reduction of Pd ions and the formation of Pd-based nanostructures.

Following the reduction step, the resulting dispersion was transferred into a Teflon-lined stainless-steel autoclave and subjected to hydrothermal treatment at an elevated temperature (160°C) for 3 h. After completion of the hydrothermal process, the autoclave was allowed to cool naturally to room temperature. The obtained dark-colored solution was centrifuged at high speed (15,000 rpm) for 20 min to remove larger particles and impurities. The supernatant containing PQDs was collected and further purified, if necessary, via dialysis or filtration. The obtained PQDs were readily dispersible in water, forming a stable and homogeneous colloidal solution without visible aggregation. Finally, the purified PQDs were stored at 4°C for subsequent characterization and incorporation into PVA nanocomposite films.

3. Preparation of PVA/PQDs Films

A 10 wt.% aqueous poly(vinyl alcohol) (PVA) solution was prepared by dissolving PVA powder in distilled water at 90 °C under continuous magnetic stirring for 1 h until a clear and homogeneous solution was obtained. The solution was then cooled to room temperature prior to further use. The PQD suspension was subsequently added to the PVA solution at different loadings (0.1, 0.5, 0.7, and 1.0 wt.% relative to the weight of PVA). The mixtures were stirred continuously for 2 h to achieve a homogeneous distribution of PQDs within the polymer matrix. The prepared nanocomposite solutions were cast onto clean, leveled glass plate and dried in a controlled environment at 40–50 °C for 48 h to allow slow solvent evaporation and uniform film formation. After drying, the films

were carefully peeled off and conditioned at 25°C and 50% relative humidity for at least 48 h prior to characterization.

The thickness of the obtained films was measured using a digital micrometer at five different random positions, and the average thickness was found to be in the range of approximately 90-100 μm. The selected PQD loading range was designed to investigate the concentration-dependent effects on the optical, antibacterial, and barrier properties of the films while minimizing the risk of nanoparticle agglomeration at higher concentrations.

4. Characterization

The morphology and size distribution of the synthesized PQDs were examined using transmission electron microscopy (TEM) (JEM-2100F, JEOL). For sample preparation, a dilute dispersion of PQDs was drop-cast onto a carbon-coated copper grid and allowed to dry naturally at room temperature prior to imaging.

The chemical structure and intermolecular interactions of the films were analyzed using attenuated total reflection Fourier-transform infrared (ATR-FTIR) spectroscopy (Perkin-Elmer Frontier FTIR). Spectra were collected over the wavenumber range of 4000-400 cm^{-1} with 64 scans at a suitable resolution, using air as the background reference.

Crystalline characteristics of the prepared films were investigated by X-ray diffraction (XRD) analysis using a Rigaku diffractometer (Ultima IV) with Cu Kα radiation (λ = 0.154 nm). The diffraction patterns were recorded over an appropriate 2θ range, and the intensities were normalized to enable comparison between samples.

Mechanical properties, including tensile strength and elongation at break, were determined using a universal testing machine (UTM, Qmesys Co., South Korea) under standard testing conditions.

The oxygen barrier performance of the films was evaluated by measuring the oxygen transmission rate (OTR) using an OX-TRAN 702 system (MOCON, USA). Film thickness was measured at multiple points using a digital thickness gauge, and the average value was used for calculations.

The antibacterial activity of the nanocomposite films was assessed against *Staphylococcus aureus* (ATCC 6538) following a disk diffusion method based on JIS Z 2801:2010. A bacterial suspension equivalent to 0.5 McFarland standard (approximately 1×10^8 CFU/mL) was prepared and uniformly spread onto tryptic soy agar plates. Sterilized circular film specimens (25 mm in diameter) were then placed onto the inoculated agar surface and incubated at 37°C for 24 h. After incubation, the diameter of the inhibition zones formed around the samples was measured using a digital caliper. All experiments were conducted in triplicate, and the results were expressed as mean values with corresponding standard deviations.

5. Statistical Analysis

All experiments were performed in triplicate, and the results are presented as mean ± standard deviation (SD). Statistical analysis was carried out using OriginPro (OriginLab Corporation, USA). Differences between samples were evaluated using one-way analysis of variance (ANOVA), followed by Tukey's post hoc test to determine significant differences between groups. A p-value of less than 0.05 ($p < 0.05$) was considered statistically significant.

Results and Discussion

1. Morphological Analysis of the Synthesized PQDs

The structural features and morphology of the synthesized PQDs were investigated using transmission electron microscopy (TEM) and high-resolution TEM (HR-TEM). As illustrated in Figure 1a, the PQDs exhibited a well-dispersed, nearly spherical morphology with good uniformity, indicating effective control over particle formation during synthesis. The good aqueous dispersibility of PQDs facilitates their uniform

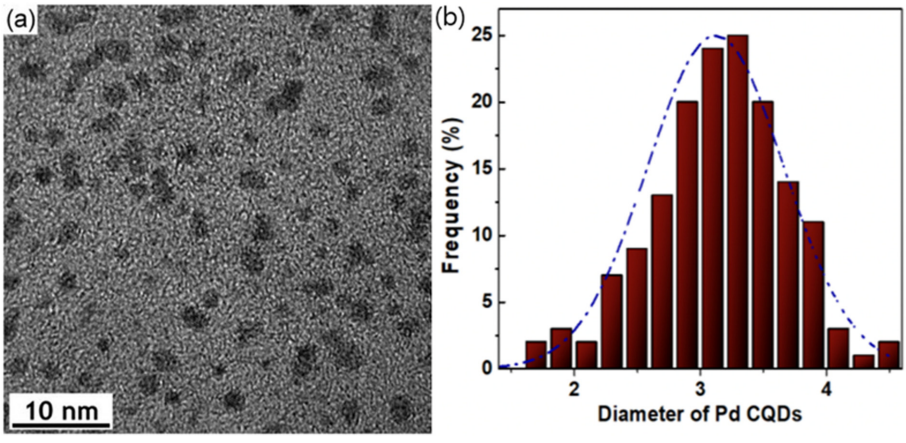

Fig. 1. (a) TEM of PQDs with 10 nm magnification and (b) particle size distribution histogram

distribution within the PVA matrix, contributing to improved optical and barrier properties.

Detailed structural analysis using HR-TEM revealed distinct lattice fringes with an interplanar spacing of approximately 0.21 nm, which can be attributed to the graphitic carbon structure, along with the possible contribution of palladium incorporation within the carbon matrix. The particle size distribution histogram (Figure 1b) demonstrates that the PQDs are predominantly below 10 nm in diameter, with an average particle size in the range of 3–4 nm. This narrow size distribution highlights the successful synthesis of nanoscale quantum dots with controlled dimensions, which is beneficial for enhancing their optical and antibacterial properties(Azam et al., 2021; Liu et al., 2025; Setianto et al., 2024).

1. Structural Analysis of PVA/PQD Nanocomposite Films

Figure 2 illustrates the FTIR spectra of pristine PVA and PVA/PQD nanocomposite films containing different PQD loadings (0.1, 0.5, 0.7, and 1.0 wt.%). The spectra were collected over the wavenumber range of 4000–500 cm^{-1}. All samples display the typical absorption features of PVA, including a broad band centered around 3300 cm^{-1}, which is attributed to O–H stretching vibrations associated with strong intermolecular and intramolecular hydrogen bonding. The peaks observed near 2940 cm^{-1} and 2850 cm^{-1} correspond to asymmetric and symmetric stretching vibrations of C–H groups, while the band at approximately 1430 cm^{-1} is assigned to CH_2 bending. Additionally, the peak located around 1090 cm^{-1} is characteristic of C–O stretching vibrations within the polymer backbone. Upon incorporation of PQDs, noticeable yet subtle modifications in the spectral features are observed. In particular, the O–H stretching band becomes broader and slightly more intense with increasing PQD content, indicating strengthened hydrogen-bonding interactions between the hydroxyl groups of PVA and the oxygen-containing functional groups present on the surface of PQDs. Furthermore, minor changes in the intensity of bands associated with C–O and C=O vibrations suggest the contribution of surface functionalities of the PQDs, such as hydroxyl, carbonyl, and carboxyl groups.

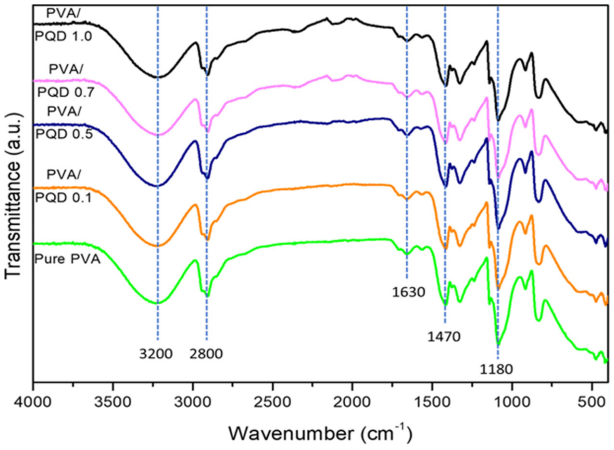

Fig. 2. FT-IR spectra of PVA/PQDs nanocomposite films.

No significant shift or emergence of distinct new peaks related to palladium species is observed, likely due to their low concentration and uniform dispersion within the polymer matrix. However, the absence of major spectral changes and the preservation of the characteristic PVA peaks confirm good compatibility between PVA and PQDs. These results indicate that the nanofillers are well incorporated into the polymer network without disrupting its fundamental chemical structure, while promoting intermolecular interactions that are beneficial for enhancing film properties(M. Jalilian et al., 2023; M. Jozaghkar et al., 2022, 2019; Mohammad Jozaghkar and Ziaee, 2024; Mohammadreza Jozaghkar and Ziaee, 2024; Kim et al., 2025).

2. Optical Properties and UV-Blocking Performance

The UV–Vis transmittance spectra of pure PVA and PVA/PQD nanocomposite films with varying PQD loadings are presented in Figure 3. The spectra were recorded over the wavelength range of 200–800 nm to evaluate the optical transparency and UV-shielding capability of the films. Pure PVA exhibited high transparency across the entire visible region, with transmittance approaching ~100% at 660 nm, indicating its excellent optical clarity but poor resistance to ultraviolet radiation. In contrast, the incorporation of PQDs significantly reduced transmittance in the UV region (200-400 nm), demonstrating enhanced UV-blocking performance. Notably,

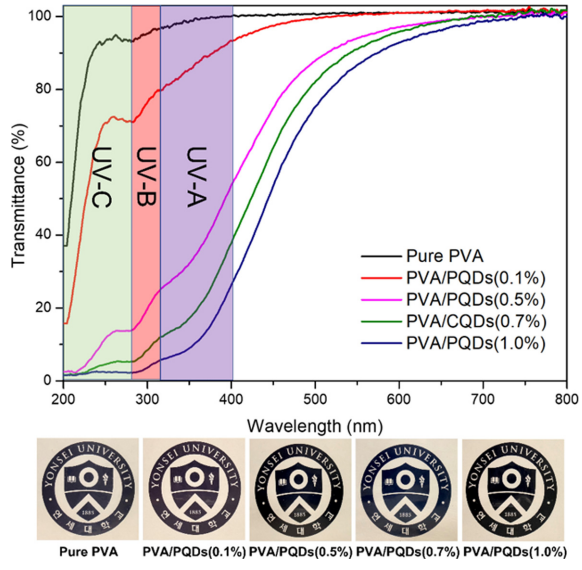

Fig. 3. (a) UV-spectra and (b) appearance of PVA/PQDs nanocomposite films.

the nanocomposite films achieved nearly complete blocking in the UV-B region (280–315 nm) and substantial attenuation in the UV-A region (315–400 nm), with blocking efficiency reaching approximately 90% at higher PQD loadings.

The improvement in UV-shielding behavior can be attributed to the strong absorption characteristics of PQDs, which arise from π–π* transitions of the carbon core and possible n–π* transitions associated with surface functional groups. Additionally, the presence of palladium species may contribute to enhanced photon absorption and scattering, further improving the UV-blocking efficiency of the films. As the PQD content increased from 0.1 to 1.0 wt.%, a gradual decrease in transmittance within the UV region was observed, indicating a concentration-dependent enhancement in UV protection. Despite this reduction in UV transmittance, the films maintained high transparency in the visible region. Specifically, the transparency at 660 nm remained above 95% even at the highest PQD loading, suggesting that the incorporation of PQDs does not significantly compromise the optical clarity of the films. This balance between excellent UV-blocking capability and high visible light transparency is particularly advantageous for food packaging applications, where protection against photo-induced degradation must be achieved without sacrificing product visibility. The results confirm that PQDs act as effective multifunctional nanofillers, enabling the development of advanced packaging materials with improved light-barrier properties.

The significant achievement in this study is achieving stunning UV-A blocking in very low PQDs concentration among other reported studies. For instance, our previous study showed that PVA nanocomposites based on tea leaf–derived CQDs showed that UV-A blocking can be achieved at CQDs concentrations higher that 1.0 wt. %. Moreover, maximum UV-A blocking was observed for the sample containing 3.0 wt.% of CQDs around 70 %. While current project demonstrates that 90% UV-A blocking can be achieved by just 0.1 wt. % of PQDs. Table 1 clearly compares current data with our previous studies(Ansari et al., 2025a; Department of Packaging & Logistics, Yonsei University et al., 2025).

3. XRD analysis of PVA/PQDs nanocomposite films

The X-ray diffraction patterns of neat PVA and PVA/PQDs nanocomposite films with different PQD loadings are shown in Figure 4. The measurements were carried out over a 2θ range of 3°–60° to examine the structural organization and crystallinity of the films. Pure PVA displays a characteristic broad diffraction peak centered at approximately 19.5°, which is commonly associated with its semi-crystalline nature, arising from the partial ordering of polymer chains embedded within an amorphous matrix. This broad feature reflects the dominance of disordered regions alongside limited crystalline domains.

Upon incorporation of PQDs, the overall diffraction profile remains largely unchanged, with the main peak at ~19.5° clearly retained in all nanocomposite samples. This indicates that the fundamental crystalline structure of PVA is preserved after the addition of PQDs. However, a gradual increase in peak intensity is observed with increasing PQD content, suggesting a slight enhancement in the degree of crystallinity. This behavior can be attributed to the nucleating effect of PQDs, which may promote more ordered packing of PVA chains during film formation. No additional sharp diffraction peaks corresponding to crystalline palladium or separate PQD phases are detected, which can be explained by their low concentration and homogeneous dispersion within the polymer matrix. This absence of distinct secondary phases confirms that the PQDs are well integrated into the PVA network without phase separation or aggregation(El-Shamy and Zayied, 2020; Gupta et al., 2009; Latif et al., 2024).

4. Oxygen barrier performance of PVA/PQDs nanocomposite films

The oxygen transmission rate (OTR) of pure PVA and PVA/PQDs nanocomposite films is summarized in Table 2. The films exhibited comparable thicknesses in the range of approximately 97-99 μm, ensuring reliable comparison of barrier performance across all samples. Pure PVA showed an OTR value of 5.54 ± 0.8 cc/m²·day, indicating moderate resistance to oxygen permeation, which is typical for hydrophilic, semi-crystalline polymers. Upon incorporation of PQDs, a substantial decrease in OTR was observed, demonstrating a clear improvement in oxygen barrier properties. Specifically, the OTR decreased to 1.84 ± 0.3, 1.23 ± 0.3, 1.08 ± 0.2, and 0.86 ± 0.1 cc/m^2·day for PQD loadings of 0.1, 0.5, 0.7, and 1.0 wt.%, respectively. This progressive reduction in oxygen permeability with increasing PQD content suggests a strong

Table 1. Comparison of UV-blocking performance of this study with our previous studies related to PVA/CQDs nanocomposite films

System	Optimum percentage (wt.%)	UV-Blocking Performance	Reference
PVA/PQDs	1	UV-A blocking (>90%)	This study
PVA/Tea Leaf-CQDs	3	UV-A blocking (～70%)	(Department of Packaging & Logistics, Yonsei University et al., 2025)
PVA/N-doped CQDs	1	UV-C blocking	(Kim et al., 2025)
PVA/Ag-NCQDs	1	UV-B blocking	(Ansari et al., 2025a)

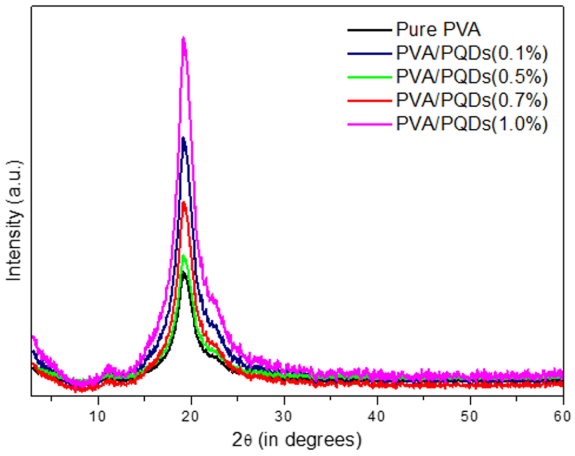

Fig. 5. XRD graph of PVA/PQDs nanocomposite films.

concentration-dependent barrier enhancement. The improvement can be primarily attributed to the homogeneous dispersion of PQDs within the PVA matrix, which introduces a more tortuous diffusion pathway for oxygen molecules. As a result, gas molecules must travel a longer and more complex route through the film, effectively reducing their transmission rate.

In addition, the slight increase in the degree of crystallinity (X_c) observed with higher PQD incorporation may further contribute to the enhanced barrier performance. Increased crystallinity typically reduces the free volume within the polymer matrix, limiting the mobility of gas molecules and thereby improving resistance to permeation. The minimal variation in film thickness among the samples indicates that thickness effects on OTR are negligible, and the observed improvements are mainly due to structural modifications induced by PQDs. Overall, these findings demonstrate that the incorporation of PQDs significantly enhances the oxygen barrier properties of PVA films, making them promising candidates for active food packaging applications where controlled oxygen permeability is essential for extending product shelf life(Ansari et al., 2025b; Chen et al., 2020; Oh et al., 2024).

Table 2. Film thickness, crystallinity degree, and oxygen barrier characteristics of PVA/PQDs nanocomposite films

	Film Thickness (mm)	Crystallinity (X_c, %)	OTR (cc/m^2.day)
Pure PVA	97 ± 1	28.6 ± 0.3	5.54 ± 0.8
PVA/PQDs (0.1%)	99 ± 2	29.7 ± 0.5	1.84 ± 0.3
PVA/PQDs (0.5%)	99 ± 1	30.9 ± 0.5	1.23 ± 0.3
PVA/PQDs (0.7%)	98 ± 2	31.8 ± 0.6	1.08 ± 0.2
PVA/PQDs (1.0%)	97 ± 3	32.9 ± 0.7	0.86 ± 0.05

*Values are expressed as mean standard deviation (n = 3)

5. Antibacterial Performance

The antibacterial performance of pure PVA and PVA/PQDs nanocomposite films was evaluated against both Gram-positive (*S. aureus*) and Gram-negative (*E. coli*) bacteria using the disk diffusion method. The quantitative measurements and example qualitative inhibition zones and corresponding quantitative measurements are presented in Figure 4. Pure PVA films exhibited negligible antibacterial activity against both tested strains, as evidenced by the absence of a clear inhibition zone, confirming that PVA itself does not possess inherent antimicrobial properties. In contrast, the incorporation of PQDs resulted in a significant improvement in antibacterial

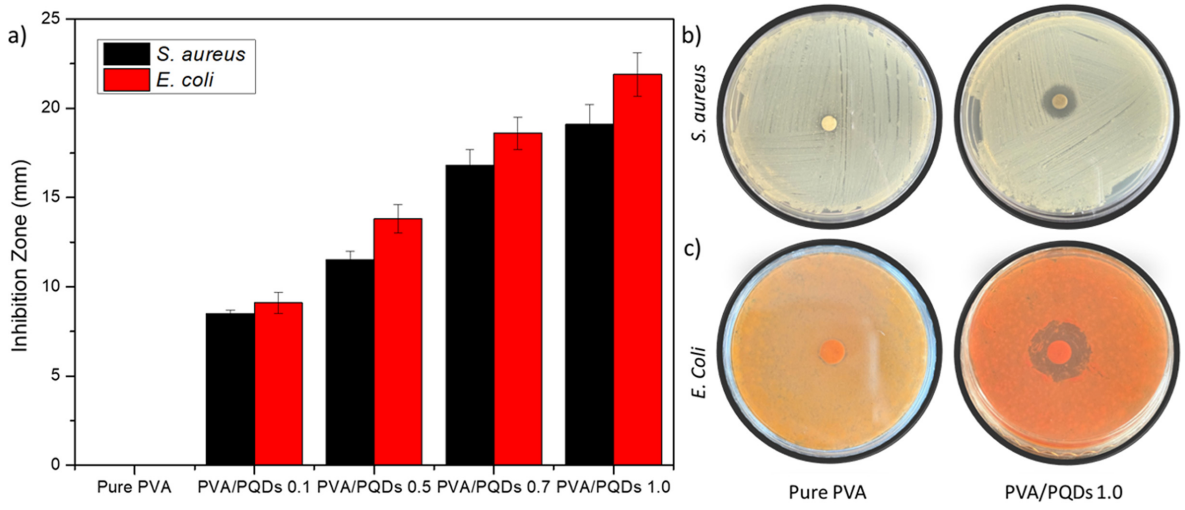

Fig. 5. Antibacterial activity of PVA/PQDs nanocomposite films: a) quantitative measurements, b and c) qualitative measurements for pure PVA and PVA/PQDs (1.0%) in *S. aureus* and *E. coli*, respectively. Error bars represent standard deviation from three independent measurements (n = 3).

Table 3. Comparison of antibacterial activity against *S. aureus* between two different CQD-based systems

System	CQDs Concentration	Inhibition Zone (mm)	Reference
PVA/PQDs	0.1	8.5 ± 0.2	This study
	0.5	11.5 ± 0.5	
	0.7	16.8 ± 0.9	
	1	19.1 ± 1.1	
PVA/Tea Leaf-CQDs	0.5	11.4	(Department of Packaging & Logistics, Yonsei University et al., 2025)
	1.0	12.9	
	2.0	16.8	
	3.0	20.5	

*Values are expressed as mean standard deviation (n = 3)

performance, with clear inhibition zones observed around the nanocomposite films.

As the PQD loading increased from 0.1 to 1.0 wt.%, the diameter of the inhibition zones progressively enlarged for both *S. aureus* and *E. coli*, indicating a concentration-dependent antibacterial effect. At the highest loading (1.0 wt.%), the inhibition zones reached approximately 19.1 ± 1.1 mm for *S. aureus* and 21.9 ± 1.2 mm for *E. coli*, demonstrating strong antimicrobial activity. Notably, the nanocomposite films showed slightly higher inhibition against *E. coli* compared to *S. aureus*, which may be attributed to differences in cell wall structure and susceptibility to reactive species. PQDs are known to generate reactive oxygen species (ROS), which can induce oxidative stress, damage bacterial cell membranes, and disrupt intracellular components. Additionally, the small size and high surface area of PQDs facilitate close interaction with microbial cells, further contributing to membrane disruption and leakage of cellular contents(Mou et al., 2023; Wang et al., 2022; Wen et al., 2025).

Surprisingly, these results were achieved by a very low concentration of PQDs. In comparison to our recent study on tea leaf-derived CQDs, it has been observed that reaching an inhibition zone of nearly 20 mm requires 3 wt.% of CQDs (Table 3)(Department of Packaging & Logistics, Yonsei University et al., 2025). Thus, introducing PQDs and improving the synthesis protocol of preparation of quantum dots significantly improves the antibacterial properties of PVA nanocomposite films.

Moreover, the observed dose-dependent behavior and broad-spectrum activity against both Gram-positive and Gram-negative bacteria highlight the potential of these nanocomposite films for use in active food packaging applications, where microbial inhibition is essential for extending shelf life and ensuring food safety.

Conclusion

In this study, PVA-based nanocomposite films reinforced with PQDs were successfully developed using a simple and effective synthesis approach. The incorporation of PQDs significantly enhanced the overall performance of PVA films without compromising their intrinsic structural integrity. The nanocomposite films exhibited outstanding UV-shielding capability, achieving near-complete blocking in the UV-B region and substantial attenuation in the UV-A region while maintaining high transparency in the visible range. Structural analysis confirmed that PQDs were well dispersed within the PVA matrix and contributed to a slight increase in crystallinity, which positively influenced the material properties. In addition, the oxygen barrier performance was markedly improved, with the OTR reduced by more than 80% compared to pure PVA, owing to the formation of a tortuous pathway and reduced molecular mobility. Importantly, the incorporation of PQDs imparted strong antibacterial activity against both Gram-positive and Gram-negative bacteria. The films demonstrated significant inhibition against *S. aureus* and *E. coli*, achieving inhibition zones of 19.1 mm and 21.9 mm, respectively, at a low filler loading of 1.0 wt.%. This highlights the high antibacterial efficiency of PQDs compared to conventional CQD systems. These synergistic properties make this system highly promising candidates for next-generation sustainable and active food packaging applications.

Acknowledgements

This study was supported by the National Research Foundation of Korea (NRF) grant funded by the Korea government (MSIP) [grant number RS-2023-00208596]. This study was also supported by the Regional Innovation System & Education (RISE) program through the Gangwon RISE Center, funded by the Ministry of Education (MOE) and the Gangwon State, Republic of Korea (2026-RISE-10-006).

References

1. Ansari, J.R., Park, K., Sadeghi, K., Seo, J., 2025. Preparation of MoS2 modified with carbon quantum dots and its application to extremely high oxygen-barrier nanocomposite

films for packaging. Food Packaging and Shelf Life 49, 101504.
2. Ansari, J.R., Park, K., Seo, J., 2025b. Improving the oxygen barrier properties of composite films using green tea extracted CQDs and PVA for active packaging applications. Food Packaging and Shelf Life 48, 101460.
3. Azam, N., Najabat Ali, M., Javaid Khan, T., 2021. Carbon Quantum Dots for Biomedical Applications: Review and Analysis. Front. Mater. 8, 700403.
4. Chen, S., Liu, D., Qian, M., Xu, L., Li, Y., Sun, H., Wang, X., Zhou, H., Bao, J., Xu, C., 2020. Preparation of cyanobacteria-enhanced poly(vinyl)alcohol-based films with resistance to blue-violet light / red light and water. PLoS ONE 15, e0228814.
5. Department of Packaging & Logistics, Yonsei University, Jozaghkar, M., Ansari, J.R., Seo, J., 2025. PVA /Tea Leaf–Derived Carbon Quantum Dots Nanocomposites for Enhanced Barrier and Antimicrobial Food Packaging Films.
6. Korean Journal of Packaging Science and Technology 31, 195-201.
7. El-Shamy, A.G., Zayied, H.S.S., 2020. New polyvinyl alcohol/carbon quantum dots (PVA/CQDs) nanocomposite films: Structural, optical and catalysis properties. Synthetic Metals 259, 116218.
8. Elugoke, S.E., Uwaya, G.E., Quadri, T.W., Ebenso, E.E., 2024. Carbon Quantum Dots: Basics, Properties, and Fundamentals, in: Berdimurodov, E., Verma, D.K., Guo, L. (Eds.), ACS Symposium Series. American Chemical Society, Washington, DC, pp. 3-42.
9. Gholizadeh, Z., Aliannezhadi, M., Ghominejad, M., Shariatmadar Tehrani, F., 2026. The novel alumina/CQDs nanocomposites for modifying optical and structural properties of alumina nanostructure. Sci Rep 16, 4837.
10. Gupta, S., Pramanik, A.K., Kailath, A., Mishra, T., Guha, A., Nayar, S., Sinha, A., 2009. Composition dependent structural modulations in transparent poly(vinyl alcohol) hydrogels. Colloids and Surfaces B: Biointerfaces 74, 186-190.
11. Jailani, A., Hidzer, M.H., Firdaus, A.H.M., Sapuan, S.M., Zainudin, E.S., Atiqah, A., Wan Jaafar, W.M., Suryanegara, L., 2026. Enhancing polyvinyl alcohol (PVA) nanocomposites: Key properties, applications and challenges in advanced engineering. Defence Technology 55, 11-29.
12. Jalilian, M., Jozaghkar, Mohammad, Ziaee, F., 2023. Novel insight into low-temperature performance of various polyalkyl methacrylate) homopolymers in lube oil. Polyolefins J. Jalilian, S.M., Jozaghkar, M.R., Ziaee, F., 2023. Synthesis and characterization of butyl methacrylate/1-hexene copolymers catalyzed by AlCl3 and organometallic acids and their performance assessment in lube oil. JPSE 6, 4957.
13. Jozaghkar, M., Han, S., Park, K., Ansari, J.R., Seo, J., 2026a. Preparation and characterization of PBAT/PLA/lemon-extract quantum dots by melt extrusion for enhanced antibacterial and sustainable packaging. Applied Surface Science 730, 166308.
14. Jozaghkar, M., Jalilian, M., Ziaee, F., 2022. Synthesis and assessment of the effect of monomer feed ratio and Lewis acids on the copolymerization of Butyl methacrylate/1-octene. Polyolefins J.
15. Jozaghkar, M., Mirtaleb, F., Ansari, J.R., Irshad, M.S., Irshad, M.K., Seo, J., Arabi, H., 2026b. Tuning melt viscoelastic properties of LDPE via reactive extrusion: a dual-agent strategy using TMPTMA and Polyhexene-1. International Polymer Processing. https://doi.org/10.1515/ipp-2025-0140
16. Jozaghkar, Mohammadreza, Ziaee, F., 2024. Characterization and kinetics study of poly(α-methyl styrene) synthesized by living anionic polymerization. J Polym Res 31, 156.
17. Jozaghkar, Mohammad, Ziaee, F., 2024. Synthesis of Novel styrene-olefin triblock copolymer via living anionic polymerization. Polyolefins J. https://doi.org/10.22063/poj.2024.3544.1290
18. Jozaghkar, M., Ziaee, F., Heyran Ardakani, H., Ashenagar, S., Jalilian, M., 2019. Kinetics of High-Temperature Bulk Thermal Polymerization of Methyl Styrene. IJPST 32.
19. Jozaghkar, M.R., Jahani, Y., Arabi, H., Ziaee, F., 2019. Effect of Polyethylene Molecular Architecture on the Dynamic Viscoelastic Behavior of Polyethylene/Polyhexene-1 Blends and Its Correlation with Morphology. Polymer-Plastics Technology and Materials 58, 560-572.
20. Jozaghkar, M.R., Sepehrianazar, A., Ziaee, F., Mirtaleb, F., 2022. Preparation, assessment, and swelling study of amphiphilic acrylic acid/chitosan-based semi-interpenetrating hydrogels. Turkish Journal of Chemistry 46, 499–505.
21. Kim, H., Park, K., Ansari, J.R., Jang, J., Ahn, K., Seo, J., 2025. Enhancing physical properties of polyvinyl alcohol film using carbon quantum dots upcycled from polyethylene terephthalate waste. Materials Today Chemistry 46, 102774.
22. Latif, Z., Albargi, H.B., Khaliq, Z., Shahid, K., Khalid, U., Qadir, M.B., Ali, M., Arshad, S.N., Alkorbi, A.S., Jalalah, M., 2024. Reinforcement using undoped carbon quantum dots (CQDs) with a partially carbonized structure doubles the toughness of PVA membranes. Nanoscale Adv. 6, 1750-1764.
23. Li, Z., Che, G., Jiang, W., Liu, L., Wang, H., 2019. Visible-light-driven CQDs@MIL-125(Ti) nanocomposite photocatalyst with enhanced photocatalytic activity for the degradation of tetracycline. RSC Adv. 9, 33238–33245.
24. Liu, Y., Feng, S., Zhu, Q., 2025. The effect of CQDs' particle size on its fluorescence behavior and Cu2+ detection. Spectrochimica Acta Part A: Molecular and Biomolecular Spectroscopy 341, 126408.
25. Mahmood, A., Shi, G., Wang, Z., Rao, Z., Xiao, W., Xie, X., Sun, J., 2021. Carbon quantum dots-TiO2 nanocomposite as an efficient photocatalyst for the photodegradation of aromatic ring-containing mixed VOCs: An experimental and DFT studies of adsorption and electronic structure of the interface. Journal of Hazardous Materials 401, 123402.
26. Mirtaleb, F., Jozaghkar, M., Ziaee, F., 2025. Controlled Polymerization Route to Novel α-Methyl styrene – Olefin Triblock Copolymers with Tailored Architecture. Polyolefins J.
27. Mou, C., Wang, X., Liu, Y., Xie, Z., Zheng, M., 2023. A robust carbon dot-based antibacterial CDs-PVA film as a wound dressing for antibiosis and wound healing. J. Mater.

Chem. B 11, 1940-1947.
28. Oh, Y., Park, K., Ansari, J.R., Seo, J., 2024. Using a Carbon Quantum Dot Suspension as a New Solvent for Clear Hydrophobic Surface Coating on Hydrophilic PVA Films. Polymers 16, 2513.
29. Qiang, T., Han, M., Wang, X., 2020. Waterborne polyurethane/carbon quantum dot nanocomposite as a surface coating material exhibiting outstanding luminescent performance. Progress in Organic Coatings 138, 105433.
30. Qurtulen, Q., Ahmad, A., Mujahid, M., Al-Hartomy, O., Hasan, P.M.Z., 2026. Hydrothermal Synthesis and Photocatalytic Performance of CQDs/TiO_2 Nanocomposites for CIP Removal. Water Air Soil Pollut 237, 136.
31. Saeed, A., Abdulwahed, J.A.M., 2024. Development and characterization of PVA-based nanocomposites with graphene and natural quartz nanoparticles for energy storage applications. Journal of Energy Storage 98, 113138.
32. Setianto, S., Men, L.K., Bahtiar, A., Panatarani, C., Joni, I.M., 2024. Carbon quantum dots with honeycomb structure: a novel synthesis approach utilizing cigarette smoke precursors. Sci Rep 14, 1996.
33. Tang, J., Li, C., Ma, W., Ba, Z., Hu, Z., Willner, I., Wang, C., 2025. An Activatable Caged Palladium Nanocomposite for Targeted Cancer Therapy. Angew Chem Int Ed 64, e202503485.
34. Wang, M., Su, Y., Liu, Y., Liang, Y., Wu, S., Zhou, N., Shen, J., 2022. Antibacterial fluorescent nano-sized lanthanum-doped carbon quantum dot embedded polyvinyl alcohol for accelerated wound healing. Journal of Colloid and Interface Science 608, 973-983.
35. Wen, F., Su, W., Cen, L., Chen, Y., Huo, L., Zhong, H., Li, P., 2025. Natural fluorescent carbon quantum dots embedded polyvinyl alcohol/chitosan film with photoregulation and high antibacterial efficiency for infected wound healing. International Journal of Biological Macromolecules 306, 141716.
36. You, J.-L., Chen, Y.-S., Chang, C.-P., Wu, M.-Z., Ger, M.-D., 2021. Utilizing a pH-responsive palladium nanocomposite to fabricate adhesion-enhanced and highly reliable copper coating on nylon 6 fabrics. Journal of Materials Research and Technology 15, 3983-3994.

투고: 2026.03.29 / 심사완료: 2026.04.01 / 게재확정: 2026.04.06